

# Short-range structures of poly(dicarbon monofluoride), $(C_2F)_n$ , and poly(carbon monofluoride), $(CF)_n$

Yuta Sato<sup>a</sup>, Keiji Itoh<sup>b</sup>, Rika Hagiwara<sup>a,\*</sup>, Toshiharu Fukunaga<sup>b</sup>, Yasuhiko Ito<sup>a</sup>

<sup>a</sup> *Department of Fundamental Energy Science, Graduate School of Energy Science, Kyoto University,  
Sakyo-ku, Kyoto, 606-8501, Japan*

<sup>b</sup> *Research Reactor Institute, Kyoto University, Kumatori-cho, Sennan-gun, Osaka 590-0494, Japan*

## Abstract

The short-range structures of the so-called graphite fluorides, poly(dicarbon monofluoride)  $((C_2F)_n)$  and poly(carbon monofluoride)  $((CF)_n)$ , have been discussed, based on the neutron diffraction data. The C–C and C–F bond lengths in these compounds are determined to be 0.157–0.158 and 0.136 nm, respectively, which slightly differ from those previously evaluated and coincide with those found in polytetrafluoroethylene (PTFE). The structure models of  $(C_2F)_n$  (both AB-type and AA'-type) and  $(CF)_n$  have been refined so as to give the best fit of the atomic pair distribution functions calculated for them ( $G_{\text{calc}}(r)$ 's) to those experimentally observed for the compounds ( $G_{\text{obs}}(r)$ 's). Since the  $G_{\text{obs}}(r)$  of  $(C_2F)_n$  better fits to the  $G_{\text{calc}}(r)$ 's of AB-type model rather than those for AA'-type model, the latter model is ruled out. The  $a$ -lattice parameter and the C–C–C bond angle in the refined structure model of  $(CF)_n$  (0.260–0.261 nm and  $111^\circ$ , respectively) are slightly larger than those of  $(C_2F)_n$

---

\* Corresponding author. Tel.: +81-75-753-5822; fax: +81-75-753-5906.

*E-mail address:* hagiwara@energy.kyoto-u.ac.jp (R. Hagiwara).

(0.256–0.257 nm and 109–110°, respectively).

*Keywords:* A. Graphite, intercalation compounds; B. Intercalation; C. Neutron scattering; D. Crystal structure

## 1. Introduction

Direct fluorination of crystalline graphite by elemental fluorine at elevated temperatures above 623 K yields layered carbon fluorides with covalent C–F bonds such as poly(dicarbon monofluoride) ((C<sub>2</sub>F)<sub>n</sub>) and/or poly(carbon monofluoride) ((CF)<sub>n</sub>) [1,2]. The proposed structure models of these compounds are illustrated in Fig. 1. They have been considered to possess buckled sheets of sp<sup>3</sup>-hybridized carbon atoms with the C–C–C bond angles ( $\angle$  C–C–C) of close to 109°28' for a regular tetrahedral site [3–6]. It has been expected that every pair of the adjacent carbon sheets in (C<sub>2</sub>F)<sub>n</sub> are bound to each other by covalent C–C bonds to form a double-decked monolayer. The AB-type and AA'-type structure models have been proposed for this compound (Fig. 1 (a) and (b)) [6]. However, these two types of the (C<sub>2</sub>F)<sub>n</sub> structures have never been distinguished from each other by the spectroscopic and diffraction analyses previously performed for this compound.

Since (C<sub>2</sub>F)<sub>n</sub> and (CF)<sub>n</sub> prepared in most cases actually possess random stacking of the fluorinated carbon layers, their XRD patterns lack the (*hkl*) (*l* ≠ 0) peaks, and the broad, asymmetric (*hk*) peaks are observed instead [7,8]. Therefore the precise determination of the structure parameters of these compounds such as the bond lengths using the conventional Bragg diffraction patterns is quite difficult. The *a*-lattice

parameters of  $(C_2F)_n$  and  $(CF)_n$  based on the hexagonal unit cells, which correspond to the distance between the nearest pair of fluorine atoms attached on the same side of a carbon sheet, have been estimated at 0.251 and 0.253–0.257 nm, respectively [5–7]. These values indicate that fluorine atoms in  $(C_2F)_n$  and  $(CF)_n$  are closely packed and not allowed to take a typical van der Waals distance (0.270 nm) from each other on the carbon sheets. However, the C–F and C–C bond lengths ( $r_{C-F}$  and  $r_{C-C}$ ) in the fluorides have been generally expected to be 0.141 and 0.153–0.154 nm, respectively, based on the typical covalent radii of carbon and fluorine atoms (0.077 and 0.064 nm, respectively) [5,6]. On the other hand, a computation study on  $(CF)_n$  based on density functional theory has yielded in a shorter  $r_{C-F}$  and a longer  $r_{C-C}$  (0.137 and 0.155 nm, respectively) [9]. These bond lengths have never been further discussed up to now, while those in polytetrafluoroethylene (PTFE) consisting of  $sp^3$ -hybridized carbon chains and covalent C–F bonds have been determined to be 0.136 and 0.158 nm (for  $r_{C-F}$  and  $r_{C-C}$ , respectively) based on neutron diffraction experiments [10]. In the present study, the short-range structures of  $(C_2F)_n$  and  $(CF)_n$  were discussed, based on their radial distribution functions ( $RDF(r)$ 's) and atomic pair distribution functions ( $G(r)$ 's) derived from neutron diffraction data.

## 2. Experimental

### 2.1 Preparation of $(C_2F)_n$ and $(CF)_n$

Graphite powder (Union Carbide, SP-1 grade, purity 99.4 %, average particle

diameter  $1 \times 10^2 \mu\text{m}$ ) was fluorinated by elemental fluorine (0.10 MPa; Daikin Industries, purity 99.7 %) in a nickel reactor tube at 673 or 873 K in order to obtain  $(\text{C}_2\text{F})_n$  (sample F-1) or  $(\text{CF})_n$  (sample F-2), respectively. The  $(\text{CF})_n$  sample supplied by Daikin Industries (average particle diameter  $1 \mu\text{m}$ ; hereafter denoted by F-3), PTFE powder (Aldrich, average grain size  $1 \mu\text{m}$ ) and the original graphite powder were also analyzed by neutron diffraction experiments without further treatment.

## 2.2 Analyses

Elemental analyses of carbon and fluorine were performed at the Center for Organic Elemental Microanalysis of Kyoto University. XRD patterns of the powder samples charged in glass sample holders (0.5 mm thick) were obtained by means of MultiFlex (Rigaku) with  $\text{CuK}\alpha$  radiation. The average crystallite size ( $L$ ) was estimated using Scherrer's equation (1);

$$L = \frac{K\lambda}{B \cos \theta} \quad (1)$$

where  $K$ ,  $\lambda$ ,  $B$ ,  $\theta$  denote the Scherrer constant, the wavelength of  $\text{CuK}\alpha$  beam, the corrected half width of a diffraction peak and the Bragg angle, respectively. A  $K$  value of 0.9 was used for the (001) reflection while that of 1.84 was used for the (10) reflection from the two-dimensional lattice [11].

Neutron diffraction measurements were carried out in the High Intensity Total

Scattering Spectrometer (HIT-II) installed at the pulsed neutron source in the High Energy Accelerator Research Organization (KEK, Tsukuba, Japan). Each powder sample was put in a vanadium tube cell with an inner diameter of 8.0 mm and a wall thickness of 0.025 mm. Corrections of the background, absorption [12] and the multiple scattering effects [13] were made on the experimentally observed scattering data. The structure factor in the Faber-Ziman definition,  $S(Q)$  ( $Q = 4\pi\sin\theta/\lambda$ ) [14], is derived from the corrected scattering intensity,  $I(Q)$ .

$$S(Q) = \frac{I(Q) - \{\langle b^2 \rangle - \langle b \rangle^2\}}{\langle b \rangle^2}, \text{ where } \langle b^2 \rangle = \sum_i c_i b_i^2, \quad \langle b \rangle = \sum_i c_i b_i \quad (2)$$

The  $c_i$  and  $b_i$  represent the concentration and the neutron coherent scattering length of the component atoms  $i$  ( $i = \text{C or F}$ ), respectively.  $RDF(r)$  and  $G(r)$  are derived from the Fourier transformation of  $S(Q)$ .

$$RDF(r) = 4\pi r^2 \rho + \frac{2r}{\pi} \int_0^{Q_{\max}} Q(S(Q) - 1) \sin(Qr) dQ \quad (3)$$

$$G(r) = \frac{2}{\pi} \int_0^{Q_{\max}} Q(S(Q) - 1) \sin(Qr) dQ \quad (4)$$

where  $\rho$  represents the average number density of atoms. The  $S(Q)$  and the  $RDF(r)$  are also written as the weighted sum of the partial structure factors,  $S_{i-j}(Q)$ , and that of the partial radial distribution functions,  $RDF_{i-j}(r)$ , respectively ( $i-j = \text{C-C, C-F, F-F}$ ).

$$S(Q) = w_{i-j} \sum S_{i-j}(Q) \quad (5)$$

$$RDF(r) = w_{i-j} \sum RDF_{i-j}(r) \quad (6)$$

where the  $w_{i-j}$  represents the weighting factor defined by Eq. (7).

$$w_{i-j} = \frac{c_i c_j b_i b_j}{\langle b \rangle^2}. \quad (7)$$

The nearest neighbor coordination number of atoms  $j$  around an atom  $i$  ( $CN_{i-j}$ ) is derived from the peak area ( $A_{i-j}$ ) corresponding to the correlation of the nearest  $i-j$  pair in the  $RDF_{i-j}(r)$  according to Eq. (8).

$$CN_{i-j} = \frac{c_j A_{i-j}}{w_{i-j}}. \quad (8)$$

Calculation of  $G(r)$ 's for the proposed structural models of  $(C_2F)_n$  and  $(CF)_n$  was performed by the PDFFIT software [15] installed on a PC. The degree of fit of  $G(r)$  calculated ( $G_{\text{calc}}(r)$ ) to that experimentally observed ( $G_{\text{obs}}(r)$ ) was evaluated using the  $R$  value given by Eq. (9).

$$R = \left( \frac{\sum_i (G_{\text{obs}}(r_i) - G_{\text{calc}}(r_i))^2}{\sum_i (G_{\text{obs}}(r_i))^2} \right)^{1/2} \quad (9)$$

Structure models were refined so as to yield the best fit of  $G_{\text{calc}}(r)$  to  $G_{\text{obs}}(r)$  which gives the smallest  $R$  values.

### 3. Results and discussion

#### 3.1 C–F and C–C bond lengths in $(\text{CF})_n$ and $(\text{C}_2\text{F})_n$

Figure 2 shows the XRD patterns of the layered carbon fluorides F-1, F-2 and F-3. The absence of the  $(hkl)$  ( $l \neq 0$ ) diffraction peaks and the asymmetric profiles of the  $(hk)$  peaks in these patterns are typical of the structures with random layer stacking. The structure parameters such as interlayer distances ( $I_c$ ), the  $a$ -lattice parameters, the average crystallite sizes along the  $c$ - and  $a$ -axes ( $L_c$  and  $L_a$ , respectively) estimated from the XRD patterns are listed together with the F/C atomic ratios in Table 1. In this table, “ $X(hk(l))$ ” ( $X = I_c, a, L_c$  and  $L_a$ ) means the parameter  $X$  determined by the  $(hk(l))$  diffraction peak. The displacement of the  $(hk)$  diffraction peaks toward larger  $2\theta$  associated with small coherent lengths [11] has been taken into account in determination of  $a(hk)$ . Precise determination of the  $a$ -lattice parameters based on the  $(hk)$  diffraction peaks seems to be quite difficult. The values  $a(10)$  and  $a(11)$  estimated for F-1 disagree with each other. The  $a(10)$  determined for F-2 slightly differ from that of F-3 although both of these samples are  $(\text{CF})_n$ . The  $(\text{C}_2\text{F})_n$  samples actually contain small  $(\text{CF})_n$ -like domains in addition to trace of peripheral  $>\text{CF}_2$  groups on the surface, as is suggested by the F/C ratios of larger than stoichiometric value of the compound, 0.50 [7]. However, such domains in the sample F-1 are too small and dispersed to be detected by

XRD. A smaller  $I_c$  and larger crystallite sizes observed for the sample F-2 indicate a higher crystallinity than that of F-3. The F/C ratios of larger than 1.0 determined for these  $(CF)_n$  samples suggest the existence of considerable amount of the peripheral  $>CF_2$  groups in these fluorides, which have been characterized by  $^{19}F$  and  $^{13}C$  NMR spectroscopy [16]. The weighting factors  $w_{i-j}$  of F-1, F-2 and F-3 are derived from the F/C ratios listed in Table 1 according to Eq. (7) (Table 2).

$S(Q)$ 's of the layered carbon fluorides, graphite and PTFE derived from neutron diffraction data are shown in Fig. 3. In the  $S(Q)$ 's of the layered carbon fluorides, small angle scattering intensities are strong at lower  $Q$  than that of the (001) Bragg diffraction peaks. The prominent peak found at around  $13 \text{ nm}^{-1}$  (corresponding to the  $d$  value of about 0.48 nm) in the  $S(Q)$  of PTFE is ascribed to the correlation between the  $(CF_2)_n$  chains [10]. The  $RDF(r)$ 's derived from these  $S(Q)$ 's by Eq. (3) are shown in Fig. 4. The  $RDF(r)$ 's of the layered carbon fluorides with covalent C–F bonds and puckered sheets of  $sp^3$ -hybridized carbon atoms are completely different from that of the original graphite. The peaks found in the  $RDF(r)$  of F-3 are poorly resolved compared to that for F-2, which is considered to be caused by the difference in the crystallinity between these  $(CF)_n$  samples. The prominent peak found at  $r$  of around 0.24 nm in the  $RDF(r)$  of PTFE is ascribed to the correlations of the second nearest atomic pairs such as  $\underline{F}-\underline{C}-\underline{F}$  and  $\underline{C}-\underline{C}-\underline{F}$ . The  $RDF(r)$  profile of each fluoride at  $r$  from 0.1 to 0.2 nm is separated to two Gaussian peaks corresponding to the pair correlations for C–F and C–C as shown in Fig. 5.  $CN_{C-F}$  and  $CN_{C-C}$  derived from the peak areas according to Eq. (8) are listed in Table 3, together with  $r_{C-F}$  and  $r_{C-C}$  determined by the peak positions.  $CN_{C-F}$  obtained for the four samples are close to their F/C atomic ratios. The sums  $CN_{C-F} + CN_{C-C}$  obtained for F-1, F-3 and PTFE agree with the ideal value of an  $sp^3$ -hybridized carbon

atom, 4.00, while that of F-2 is a little larger due to the overestimated  $CN_{C-C}$ . The  $r_{C-F}$  and  $r_{C-C}$  in  $(CF)_n$  almost coincide with those in  $(C_2F)_n$ , also agreeing with those found for PTFE [10]. They are close to the estimated values based on the density functional theory ( $r_{C-F} = 0.137$  nm,  $r_{C-C} = 0.155$  nm) [9] rather than to those estimated from the typical covalent radii of carbon and fluorine atoms ( $r_{C-F} = 0.141$  nm,  $r_{C-C} = 0.153\text{--}0.154$  nm) [5,6].

### 3.2 Refinement of the structure models of $(C_2F)_n$ and $(CF)_n$

The structure parameters such as the  $a$ -lattice parameters, atomic coordinates and thermal factors in the proposed structure models of  $(C_2F)_n$  and  $(CF)_n$  were refined so as to give the best fit of  $G_{\text{calc}}(r)$ 's to  $G_{\text{obs}}(r)$ 's of the samples F-1, F-2 and F-3. The parameters  $I_c$ ,  $r_{C-F}$  and  $r_{C-C}$  were fixed as they have been determined in Section 3.1, and the space symmetry of the monolayers ( $P\bar{3}m1$  for AB-type  $(C_2F)_n$  and  $(CF)_n$ ,  $P\bar{6}m2$  for AA'-type  $(C_2F)_n$  [6,8]. See Fig. 6) were maintained during the refinement. Two types of the ordered stacking sequences were assumed here to simplify the calculation of  $G_{\text{calc}}(r)$ 's, while the samples F-1, F-2 and F-3 actually possess randomly stacked layers. The type-I and type-II stacking sequences make the nearest pair of fluorine atoms on the adjacent layers take the maximum and minimum distances, respectively (Fig. 7).

$G_{\text{calc}}(r)$ 's based on the four types of the structure models for  $(C_2F)_n$  (a-I, a-II, b-I and b-II in Fig. 7) are shown in Fig. 8, compared to  $G_{\text{obs}}(r)$  of F-1. The  $R$  values of the refinement at  $r$  from 0.1 to 0.8 nm are 17.4, 21.1, 34.8 and 25.4 % for  $G_{\text{calc}}(r)$ 's based on the models of a-I, a-II, b-I and b-II, respectively. Since the contribution of the

interlayer correlations to  $G(r)$  at  $r$  below 0.5 nm is much less than that of the intralayer correlations, the profiles of  $G_{\text{calc}}(r)$ 's at such  $r$  range do not strongly depend on the type of the stacking sequences of the monolayers. On the other hand, relative intensities of the peaks found at  $r$  of 0.3–0.4 nm in  $G_{\text{calc}}(r)$ 's based on the AB-type models (a-I and a-II) clearly differ from those for AA'-type models (b-I and b-II), which is caused by the different forms of  $C_6$  rings in the unit cells (“chair” and “boat” forms for the former and the latter models, respectively. See Fig. 6).  $G_{\text{calc}}(r)$ 's of AB-type models better fit to  $G_{\text{obs}}(r)$  than those of AA'-type models, therefore it is concluded that the former type is more reasonable for the monolayer structure of  $(C_2F)_n$ .

The  $G_{\text{calc}}(r)$ 's based on the structure models of  $(CF)_n$  with type-I and type-II stacking sequences (c-I and c-II in Fig. 7, respectively) are fitted to the  $G_{\text{obs}}(r)$ 's of F-2 and F-3 in Fig. 9. The  $R$  values on the pairs of  $(G_{\text{obs}}(r), G_{\text{calc}}(r))$  at  $r$  from 0.1 to 0.6 nm are 25.8, 24.6, 32.2 and 34.8 % for (F-2, c-I), (F-2, c-II), (F-3, c-I) and (F-3, c-II), respectively. The larger  $R$  values obtained for F-3 than those for F-2 seem to be mainly caused by the larger discrepancy of  $G_{\text{calc}}(r)$ 's from  $G_{\text{obs}}(r)$  at  $r$  of around 0.24 nm. Since the structural defects in  $(CF)_n$  such as  $>CF_2$  groups are not taken into account for the calculation of  $G_{\text{calc}}(r)$ 's, the residual components given by  $G_{\text{obs}}(r) - G_{\text{calc}}(r)$  at such  $r$  are reasonably ascribed to the correlations of the second nearest atomic pairs such as  $\underline{F}-C-\underline{F}$  and  $\underline{C}-C-\underline{F}$  involving  $>CF_2$  groups. These results indicate that F-3 contains a larger amount of  $>CF_2$  groups than those in F-2, which is in accordance with the lower crystallinity of the former described in Section 3.1. At  $r$  out of around 0.24 nm,  $G_{\text{obs}}(r)$  of F-3 as well as that of F-2 is well simulated by  $G_{\text{calc}}(r)$ 's.

The structure parameters of the refined monolayers of  $(C_2F)_n$  and  $(CF)_n$  based on  $G_{\text{obs}}(r)$ 's of F-1, F-2 and F-3 are listed in Table 4. For each sample, the assumed type

of the stacking sequences does not strongly affect the refined parameters. The parameters refined for F-2 and that for F-3 agree well with each other, almost independent of the crystallinity of these  $(CF)_n$  samples with different  $I_c$ . The  $\angle F-C-C$  and  $\angle C-C-C$  in  $(CF)_n$  determined here agree with those calculated based on density functional theory ( $108.2^\circ$  and  $110.7^\circ$ , respectively) [9]. The  $\angle C-C-C$  as well as the  $a$ -lattice parameters determined for  $(CF)_n$  are a little larger than those of  $(C_2F)_n$ . Each carbon atom on the two-dimensional network of C-C bonds in  $(CF)_n$  is slightly displaced from the regular tetrahedral site with  $\angle C-C-C$  of  $109^\circ 28'$ , due to the repulsive interaction between the nearest pair of fluorine atoms, but such distortion is less likely to occur in the diamond-like rigid network of C-C bonds in  $(C_2F)_n$ .

#### 4. Conclusion

The  $r_{C-C}$ 's in  $(C_2F)_n$  and  $(CF)_n$  were determined to be 0.157 and 0.158 nm, respectively, from the  $RDF(r)$ 's obtained by neutron diffraction experiments, while the  $r_{C-F}$ 's of both the compounds were estimated at 0.136 nm. These bond lengths clearly indicate that the C-C and C-F bond characters in  $(C_2F)_n$  and  $(CF)_n$  are essentially the same as those in PTFE.  $G_{calc}(r)$ 's based on AB-type  $(C_2F)_n$  model better fit to  $G_{obs}(r)$  of the compound than those of AA'-type model, therefore the latter is ruled out. The  $a$ -lattice parameter and  $\angle C-C-C$  determined for  $(CF)_n$  (0.260–0.261 nm and  $111^\circ$ , respectively) are a little larger than those for  $(C_2F)_n$  (0.256–0.257 nm and  $109$ – $110^\circ$ , respectively). The carbon network of  $(CF)_n$  is more flexible than those in  $(C_2F)_n$  and slightly compressed so that the repulsion between the nearest pair of fluorine atoms

attached on the sheet are decreased.

## **Acknowledgement**

Dr. Shinji Kohara of Japan Synchrotron Radiation Research Institute is acknowledged for his valuable advices. A part of this work was financially supported by Kyoto University 21<sup>st</sup> Century COE Program “Establishment of COE on Sustainable Energy System.”

## **References**

- [1] Watanabe N, Nakajima T, Touhara H. Graphite Fluorides, Amsterdam: Elsevier; 1988.
- [2] Watanabe N, Nakajima T. Graphite fluorides and carbon–fluorine compounds. Boca Raton: CRC Press; 1991.
- [3] Rüdorff W, Rüdorff G. Tetrakohlenstoffmonofluorid, eine neue Graphit-Fluor-Verbindung. Chem Ber 1947;80(5):417–423.
- [4] Lagow RJ, Badachhape RB, Wood JL, Margrave JL. Some new synthetic approaches to graphite–fluorine chemistry. J Chem Soc Dalton Trans 1974;:1268–1273.
- [5] Takashima M, Watanabe N. Formation and structure of crystalline graphite fluoride. J Chem Soc Jpn 1975;(3):432–436 [in Japanese].
- [6] Touhara H, Kadono K, Fujii Y, Watanabe N. On the structure of graphite fluoride. Z

anorg allg Chem 1987;544:7–20.

[7] Kita Y, Watanabe N, Fujii Y. Chemical composition and crystal structure of graphite fluoride. *J Am Chem Soc* 1979;101:3832–3841.

[8] Fujimoto H. Structure analysis of graphite fluoride by the Rietveld method. *Carbon* 1997;35(8):1061–1065.

[9] Charlier JC, Gonze X, Michenaud JP. First-principles study of graphite monofluoride (CF)<sub>n</sub>. *Phys Rev B* 1993;47(24):16162–16168.

[10] Schwartz BR, Mitchell GR. A detailed single chain model for molten poly(tetrafluoroethylene) from a novel structure refinement technique on neutron scattering data. *Polymer* 1994;35(15):3139–3148.

[11] Warren BE. X-ray diffraction in random-layer lattices. *Phys Rev* 1941;59:693–698.

[12] Paalman HH, Pings CJ. Numerical evaluation of X-ray absorption factors for cylindrical samples and annular sample cells. *J Appl Phys* 1965;33:2635–2639.

[13] Blech IA, Averbach BL. Multiple scattering of neutron in vanadium and copper. *Phys Rev* 1965;137(4A):1113–1116.

[14] Faber TE, Ziman JM. A theory of the electrical properties of liquid metals. III. The resistivity of binary alloys. *Phil Mag* 1965;11(109):153–173.

[15] Proffen T, Billinge SJL. PDFFIT, a program for full profile structural refinement of the atomic pair distribution function. *J Appl Cryst* 1999;32(3):572–575.

[16] Krawietz TR, Haw JF. Characterization of poly(carbon monofluoride) by <sup>19</sup>F and <sup>19</sup>F to <sup>13</sup>C cross polarization MAS NMR spectroscopy. *J Chem Soc Chem Commun* 1998;:2151–2152.

Table 1

Structure parameters of the samples F-1, F-2 and F-3

Sample	Type of fluoride	$L_c(001)$ (nm)	$a(10)$ (nm)	$a(11)$ (nm)	$L_c(001)$ (nm)	$L_a(10)$ (nm)	F/C ratio
F-1	$(C_2F)_n$	0.872	0.252	0.256	2.4	46	0.696
F-2	$(CF)_n$	0.623	0.258	0.258	6.1	58	1.190
F-3	$(CF)_n$	0.711	0.260	<sup>1)</sup>	2.4	28	1.184

<sup>1)</sup> The (11) diffraction peak is too faint to determine  $a(11)$ .

Table 2

Weighting factors ( $w_{i-j}$ ) of the samples F-1, F-2 and F-3 for neutron diffraction

Sample	WC-C	WC-F	WF-F
F-1 ((C <sub>2</sub> F) <sub>n</sub> )	0.395	0.467	0.138
F-2 ((CF) <sub>n</sub> )	0.247	0.500	0.253
F-3 ((CF) <sub>n</sub> )	0.249	0.500	0.251

Table 3

Nearest neighbor coordination numbers ( $CN_{i-j}$ ) and interatomic distances ( $r_{i-j}$ ) of the fluoride samples

Sample	$CN_{C-F}$ (atoms)	$r_{C-F}$ (nm)	$CN_{C-C}$ (atoms)	$r_{C-C}$ (nm)	$CN_{C-F} + CN_{C-C}$ (atoms)
F-1 [(C <sub>2</sub> F) <sub>n</sub> ]	0.68	0.136	3.27	0.157	3.95
F-2 [(CF) <sub>n</sub> ]	1.05	0.136	3.22	0.158	4.27
F-3 [(CF) <sub>n</sub> ]	1.12	0.136	2.89	0.158	4.01
PTFE	1.98	0.135 (0.136 [10])	1.97	0.157 (0.158 [10])	3.95

Table 4

The structure parameters for the refined models of the monolayers in  $(C_2F)_n$  and  $(CF)_n$ 

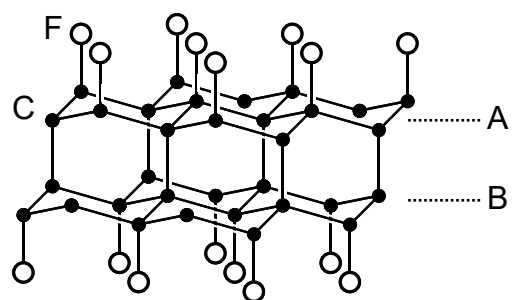
Sample ( $I_c$ / nm)	F-1 (0.872)		F-2 (0.623)		F-3 (0.711)	
Assumed stacking sequence	a-I	a-II	c-I	c-II	c-I	c-II
$a$ / nm	0.257	0.256	0.260	0.261	0.260	0.260
$I_c z_1(C_1)^{1)}$ / nm	0.078	0.078	0.025	0.024	0.025	0.025
$I_c z_2(C_2)^{1)}$ / nm	0.130	0.132	–	–	–	–
$I_c z_3(F)^{1)}$ / nm	0.266	0.268	0.161	0.160	0.161	0.161
$\angle F-C-C / ^\circ$	109	110	108	108	108	108
$\angle C-C-C / ^\circ$	110 <sup>2)</sup> , 109 <sup>3)</sup>	109 <sup>2)</sup> , 110 <sup>3)</sup>	111	111	111	111

<sup>1)</sup> Atomic coordinates of the atoms  $C_1$ ,  $C_2$  and F are given by  $(\frac{1}{2} \pm \frac{1}{6}, \frac{1}{2} \mp \frac{1}{6}, \frac{1}{2} \pm z_1)$ ,  $(0,$

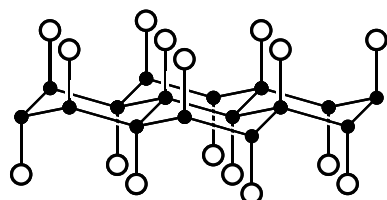
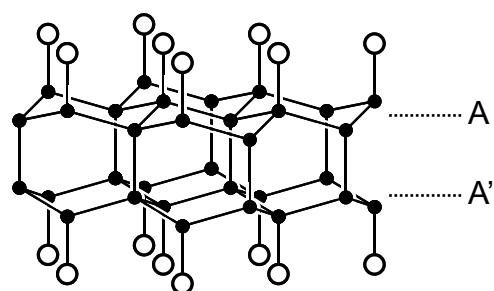
$0, \frac{1}{2} \pm z_2)$  and  $(\frac{1}{2} \pm \frac{1}{6}, \frac{1}{2} \mp \frac{1}{6}, \frac{1}{2} \pm z_3)$ , respectively.

<sup>2)</sup>  $\angle C_1-C_2-C_1'$ ,  $\angle C_2-C_1-C_2'$

<sup>3)</sup>  $\angle C_2-C_1-C_1'$



a: AB-type  $(C_2F)_n$



c:  $(CF)_n$

Fig. 1. Proposed structural models of monolayers in (a) AB-type  $(C_2F)_n$ , (b) AA'-type  $(C_2F)_n$  and (c)  $(CF)_n$ .

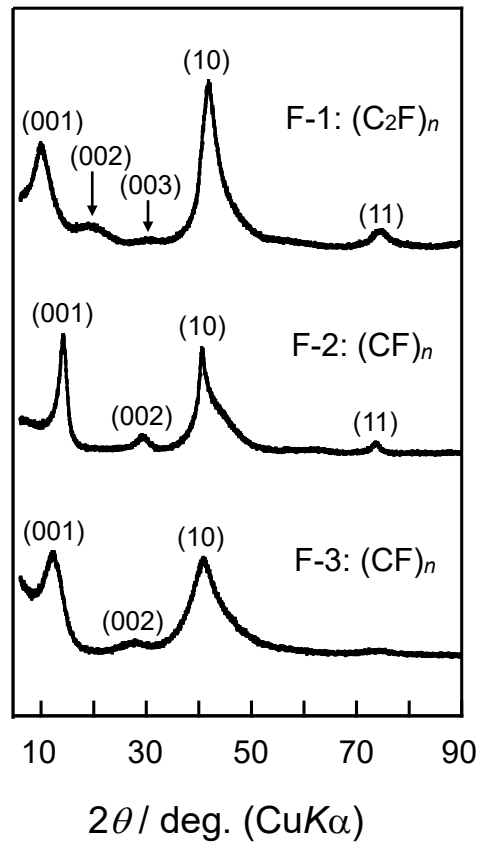


Fig. 2. XRD patterns of the samples F-1, F-2 and F-3.

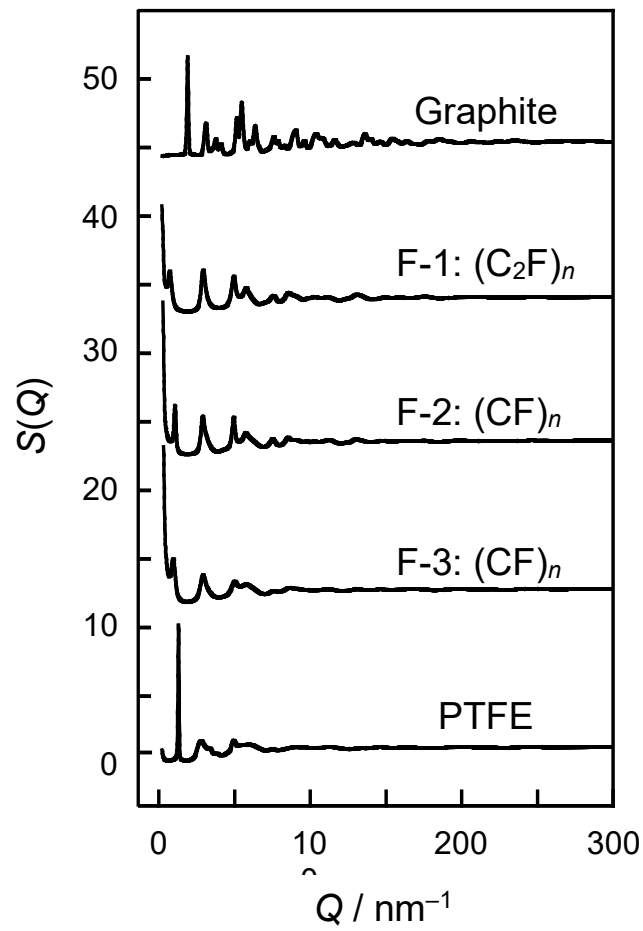


Fig. 3. The structure factors,  $S(Q)$ 's, of graphite, the samples F-1, F-2, F-3 and PTFE derived from the neutron diffraction data.

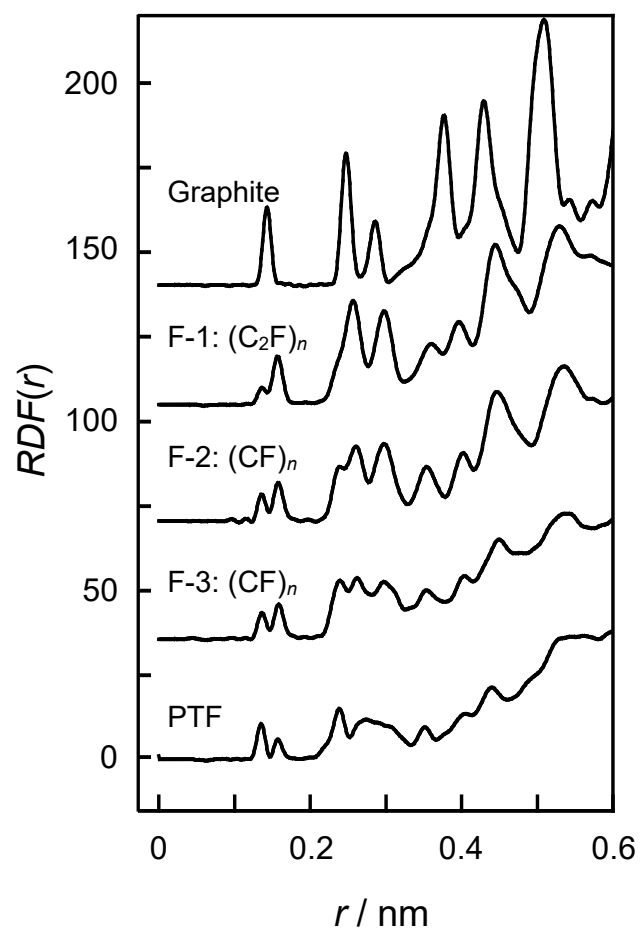


Fig. 4. Radial distribution functions,  $RDF(r)$ 's, of graphite, the samples F-1, F-2, F-3 and PTFE.

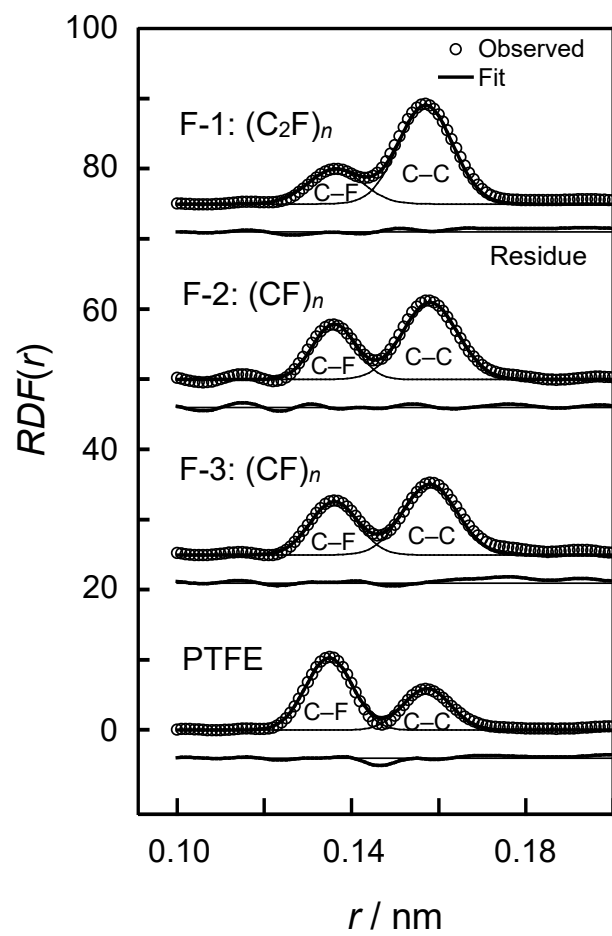


Fig. 5. Radial distribution functions,  $RDF(r)$ 's, of the samples F-1, F-2, F-3 and PTFE.

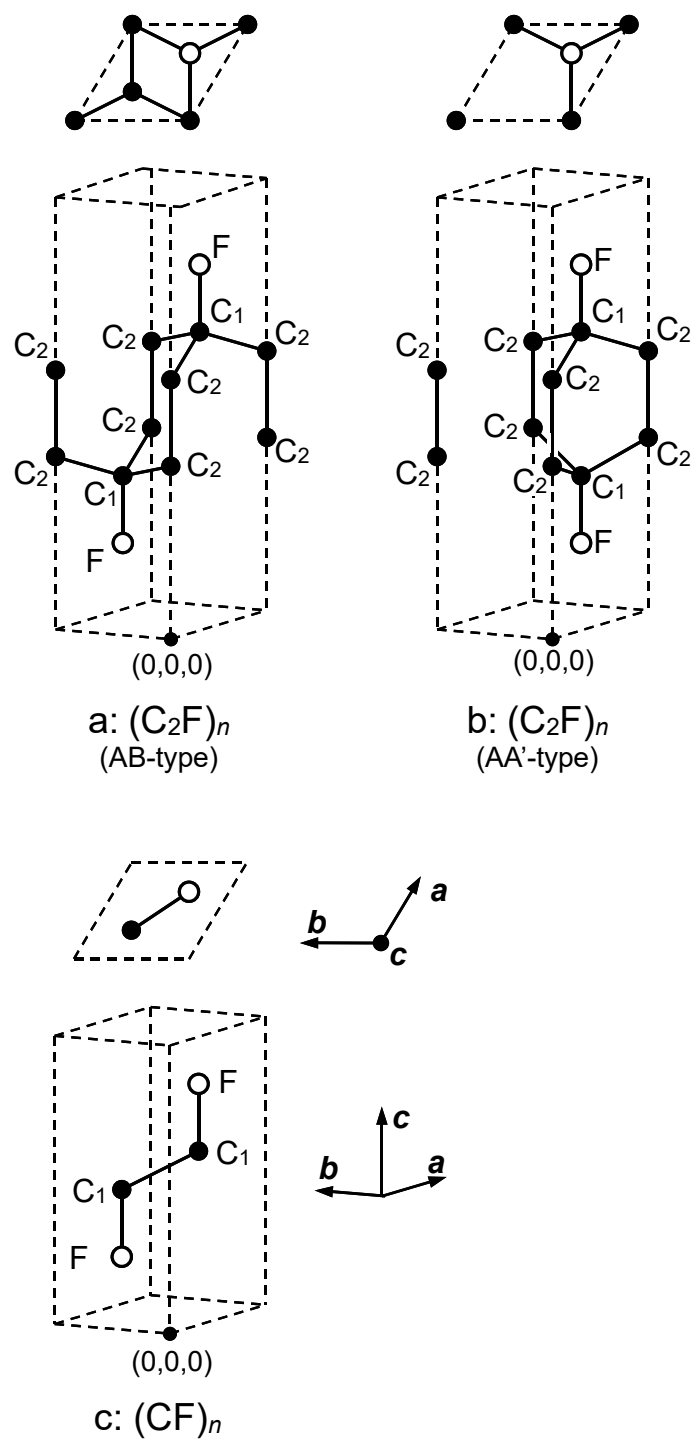


Fig. 6. The unit cells of the monolayers of (a) AB-type  $(C_2F)_n$ , (b) AA'-type  $(C_2F)_n$  and (c)  $(CF)_n$ .

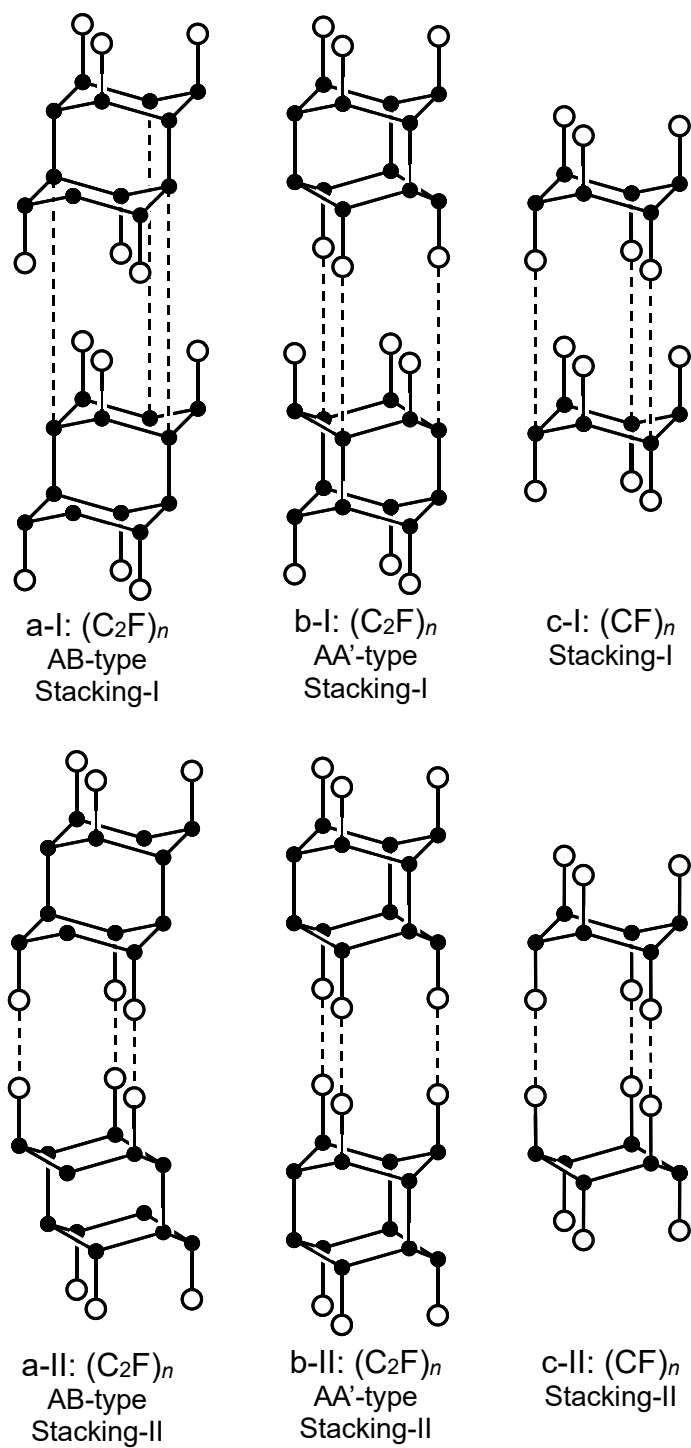


Fig. 7. The stacking sequences of the monolayers of AB-type  $(C_2F)_n$ , AA'-type  $(C_2F)_n$  and  $(CF)_n$  assumed for the  $G(r)$ -based refinement of the structure models.

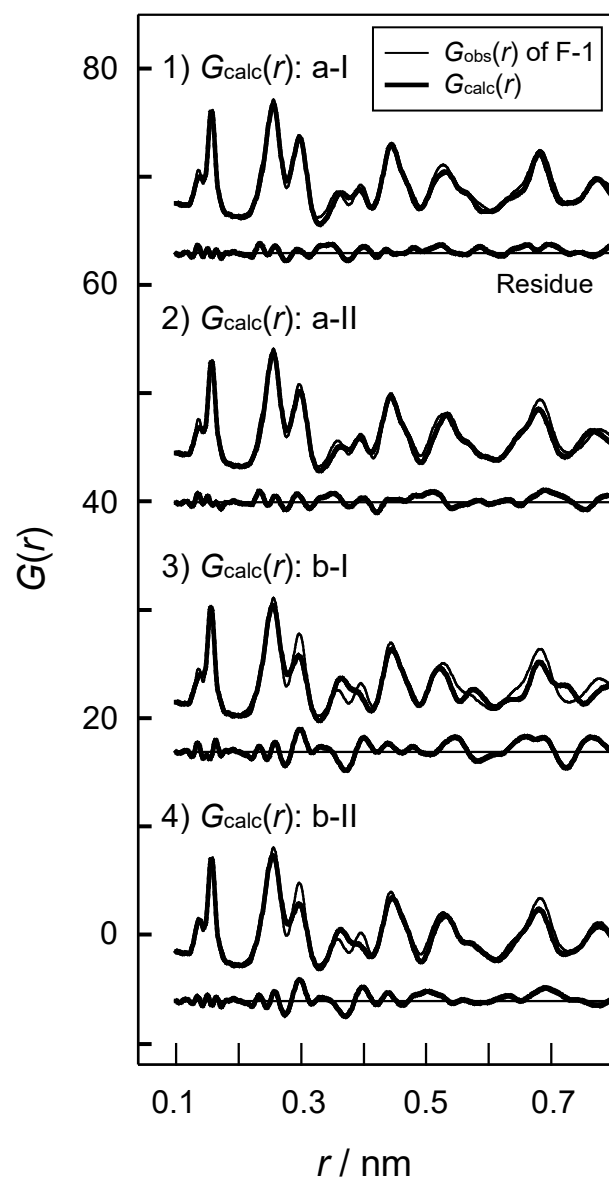


Fig. 8. Atomic pair distribution functions,  $G(r)$ 's, of the  $(\text{C}_2\text{F})_n$  structure models fitted to the curve experimentally obtained for the sample F-1.

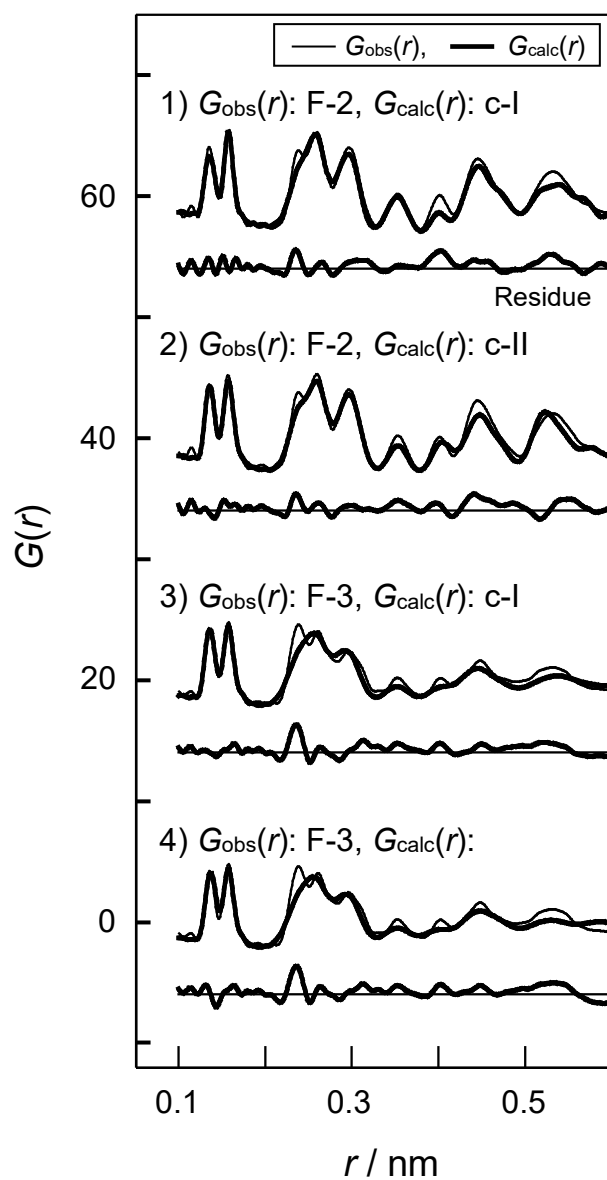


Fig. 9. Atomic pair distribution functions,  $G(r)$ 's, of the  $(\text{CF})_n$  structure models fitted to the curves experimentally obtained for the samples F-2 and F-3.